Structural and Optical Analysis of $Ti_{1-x}Co_xO_2$ (X=0.0, 0.025, 0.05, 0.075) Nanocrystalline Particles Synthesized via Sol-gel Method

Anand Kumar
Assistant Professor, Department of Physics, University College, Kurukshetra University Kurukshetra, Haryana-136119, India

Abstract

Present study focused on the concentration effect of dopant on structural and optical properties of host material. $Ti_{1-X}Co_XO_2$ for X=0.0, 0.025, 0.05, 0.075 nanocrystalline powder were synthesized using sol-gel method. Structural analysis were done by X-ray diffraction (XRD) pattern, which confirmed the phase of synthesized nanoparticles corresponds to tetragonal anatase phase of TiO_2. Also, extra peaks related any type of impurity is not observed in XRD pattern. The average crystalline size evaluated using Scherer's formula was found to be from 45 nm to 29 nm. Crystalline size and strain also calculated using Williamson–Hall analysis. Band gap decreases with doping and further increases with doping concentration.

Keywords— *TiO_2, Anatase, Williamson–Hall analysis, Band gap*

I. INTRODUCTION

Nano crystalline materials have great attention due to their versatile applications in various fields. TiO_2 is a transition metal oxide and in nano crystalline form have an excellent properties such as high stability, non-toxicity, biocompatibility etc. due to its low cost [1]. Also, it has large number of applications related to water treatment, antibacterial, sensing, medicine and self-cleaning activity. Applications and properties of TiO_2 nano crystalline strongly influenced by particle size, homogeneity, phase, porosity and surface area. It absorb light near ultraviolet region due its broad band gap (3.2 eV) and hence have no sensitivity for visible light [2]. Doping of transition metals have great influence on the properties of TiO_2 nano crystalline. Since last two decade, extensively research have been carried out on TM doped TiO_2 nano crystalline and thin films [3]-[5]. It is observed that, most of work have been focused on thin films, but only few results have been reported in literature on TM doped TiO_2 nano crystalline [6], [7]. Many attempts have been made to improve the photocatalytic activity of TiO_2 under visible-light irradiation such as doping with transition metal (Fe, Co, Ni, Cr, Mn etc) [1]-[8]. Cobalt has been preferred as a good dopant due to radius of Co^{2+} (0.65 Å) being similar to that of Ti^{4+} (0.61Å). So that, Co ions might easily be incorporated within the crystal lattice of TiO_2. Here, sol-gel method has been adopted to synthesize nano crystalline of undoped and doped TiO_2. Sol-gel method is simple, low cost, and during the synthesis doping concentration and temperature can be controlled effectively.

II. EXPERIMENTAL DETAILS

Doped and undoped TiO_2 nano crystalline powder were prepared by sol-gel method using Titanium Tetrabutoxide as a precursor and glacial acetic acid as a solvent at room temperature. Cobalt Acetate Tetrahydrate precursor was used in stoichiometry ratio for the doping of cobalt to get 2.5,5.0 and 7.5 % doping concentration. Solvent and precursors and dissolved in appropriate ratio and stirred for 1 hour. The gel obtained was dried are 80^oC in oven. The final powder was annealed in furnace at 600 ^oC for 2 hours.

The crystal structure and phase analysis of all samples were studied by X-ray diffractometer. UV–visible absorption spectra of the samples were recorded on UV-Visible Spectrometer**.**

III. RESULT AND DISCUSSION

The doped and undoped TiO_2 nanocrystalline as obtained by sol-gel technique were characterized by XRD and corresponding XRD patterns for all samples are shown in fig.1. XRD was performed for 2θ range from 20° to 80° with a step size of 0.02°. The peaks are indexed and tetragonal anatase phase is confirmed from JCPDS powder diffraction card file no. 73-1764. Almost, similar structure is observed for all samples. This indicates that uniform distribution of dopants. No extra peaks correspondence to oxide of Co is not observed which confirmed that confirmed that Co^{2+} substituted Ti^{4+} into TiO_2 lattice. Due to minor difference in ionic radii of Ti^{4+} and Co^{2+}, minor shift of most intense peaks position towards higher diffraction angle with increase in doping concentration is observed which indicating the increase in the lattice parameters and which is in agreement with previous reports on doped TiO_2 [8]-[10]. The decrease in the intensity of the XRD peaks is also observed with increase in Co^{2+} doping concentration, which might be due to increase of lattice defects in the TiO_2 with increase in dopant concentration [11].

A. *Crystalline Size*

The average crystalline size 'D' was calculated using Debye Scherrer's formula [10] i.e.

$$D = \frac{k\lambda}{\beta Cos\theta} \qquad (1)$$

where λ represents wavelength of incident beam (i.e. 1.54059 Å), β is the Full Width Half Maxima (FWHM) of the diffraction peak, k is the shape factor (i.e. 0.9) and θ represents scattering angle of reflection.

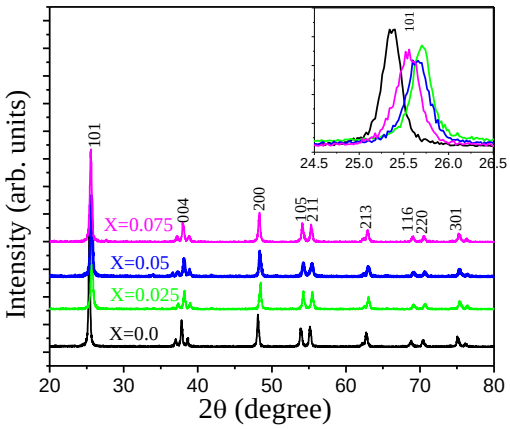

Fig.1: Powder X-Ray Diffraction Patterns of Undoped and Doped Tio_2

Using the XRD data, the lattice strain (ε) and crystalline size can also be estimated by Williamson–Hall equation [12]:

$$\beta Cos\theta = \frac{k\lambda}{D} + 4\varepsilon Sin\theta \qquad (2)$$

To evaluate the lattice strain and crystalline size, the plots of βcosθ w.r.t. 4sinθ for all samples are linear fitted (fig. 2) and the lattice strain and crystalline size are obtained from their slopes and intercepts, respectively. A negative slope in the observed plot indicates the presence of compressive strain [13], whereas the positive slope indicates tensile strain [14], [15]. Here we observed that with increase in dopant concentration tensile strain decreases upto X= 0.05 and for X=0.075 compressive strain is observed as shown in Table 1. The compressive strain for X=0.075 might be due to decrease in crystalline size.

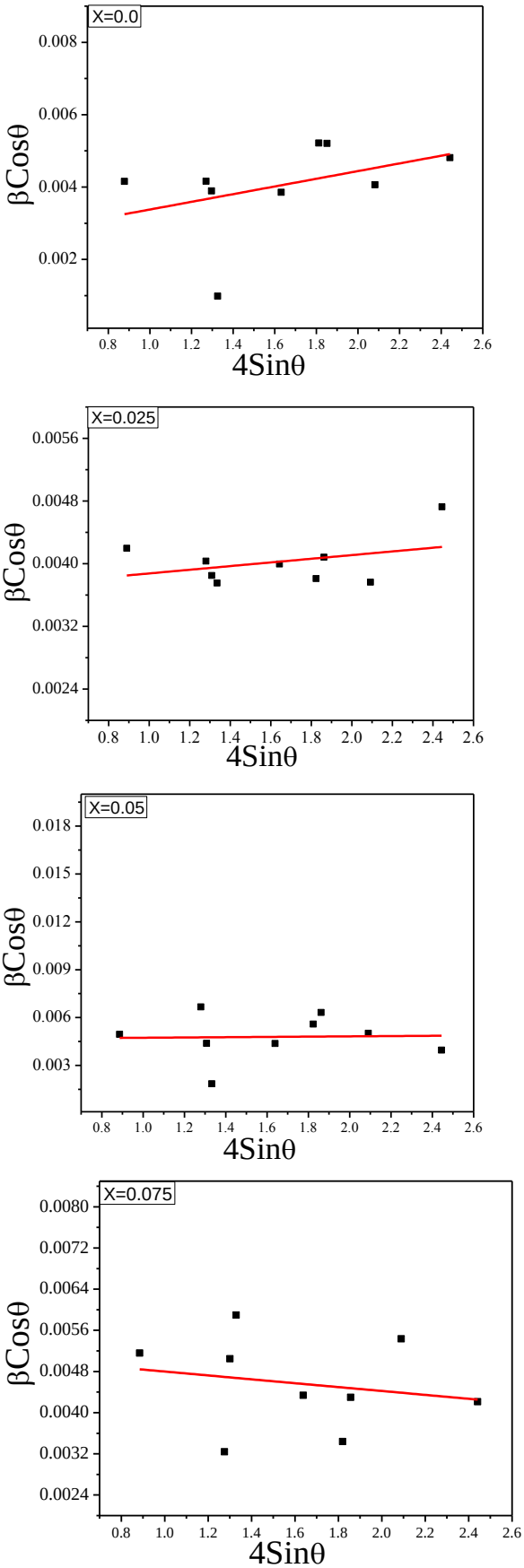

Fig. 2 Plot Of Bcosθ and 4sinθ for Undoped and Doped Tio_2

B. Specific Surface Area (SSA):

SSA is a material property and has a particular importance in case of adsorption, reactions on surfaces and photocatalysis. Mathematically, SSA can be calculated using the formula [16].

$$SSA = \frac{SA_p}{V_p * Density} \qquad (3)$$

where SAp is Surface Area and Vp is particle volume. The observed SSAs in all cases are listed in Table-1. From Table-1 it is clear that SSA increases with doping as reported in earlier reports [16, 17]. With increase in doping concentration there is further increase in SSA and hence, its applicability increases for the reactions or activities which occurs on surface and strongly depends on the surface area of the material.

C. Dislocation Density

A dislocation is a crystallographic defect within a crystal structure. The dislocation density (Δ) is the length of dislocation lines per unit volume of the crystal and has been determined using the following relation [18].

$$\Delta = \frac{1}{D^2} \qquad (4)$$

where D is crystalline size (nm). The movement of a dislocation is hindered by other dislocations present in the crystal. Thus, larger dislocation density indicates larger hardness [19]. It has been shown that the dislocation density increases while the grain size decreases with increasing strain and ultimately these parameters reach to saturation values . In our case, it is clear that Dislocation density increases while particle size decreases. It implies that the prepared doped TiO_2 nanoparticles have more strength and hardness, hence, the same increases with doping concentration.

D. Morphology Index (MI)

The applicability of nanopowder is widely used in many diverse industries, due to its unique structural, physical and chemical properties, which are reflected by its hardness, surface properties, particle size and morphology. It is proposed that the specific surface area of TiO_2 nanopowder depends on the interrelationships of particle morphology and size. MI is calculated from FWHM of XRD patterns using equation [20].

$$MI = \frac{FWHM_h}{FWHM_h - FWHM_p} \qquad (5)$$

where $FWHM_h$ and $FWHM_p$ are the highest FWHM value obtained from peaks and FWHM of particular peak for which M.I. is to be calculated, respectively. MI ranges for all samples from 0.5 to 0.59 as depicted in Table.1. It confirms the uniformity and fineness of the prepared nanoparticles

Table-1: Particle Size by Various Methods, Specific Surface Area (SSA), Dislocation Density (δ) and Morphology Index (MI) of Doped and Undoped TiO_2 Samples.

Samples	Scherrer Equation	W-H Method		SSA (nm)^2/gm	Dislocation Density (δ)	M.I.
X	D (nm)	D (nm)	Strain			
0.0	45.82	59.76	0.0011	40	0.0009	0.59
0.025	34.62	38.09	0.0002	41	0.0008	0.57
0.050	32.93	29.82	0.0001	49	0.0010	0.58
0.075	32.09	26.77	-0.0003	50	0.0011	0.56

E. Optical Properties:

The absorption spectra of all the samples were obtained from UV–vis diffuse reflectance spectroscopy. The corresponding Tauc plots $(\alpha h\nu)^2$ vs. $(h\nu)$ of all studied samples were represented in Fig. 3. The band gaps for all samples were calculated from graph using the Tauc equation [10]:

$$\alpha h\nu = A(h\nu - E_g)^2 \qquad (6)$$

where α is the absorption coefficient, hν is the photon energy and E_g is Band gap. The extrapolation of the rising part of the plots to the energy-axis given the band gap. The estimated bandgap for X=0.0, 0.025, 0.05 and 0.075, samples were found to be 3.21, 3.11, 3.09 and 2.93eV, respectively. Thus, with doping band gap can be tuned. Due to substitution replacement of Ti^{4+} by Co^{2+} in the TiO_2 lattice, as confirmed from XRD, the formation of oxygen vacancies and additional impurity band arises, resulting in absorption of visible light and narrowing of band gap [21]. Similar results are reported by Guo *et.al.* [8] for Mn-doped anatase TiO_2 , which strengthened our results.

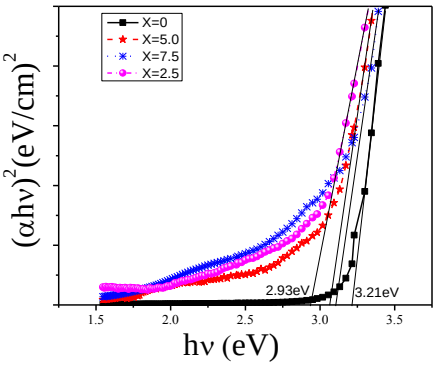

Fig. 3-Tauc Plot For Undoped, Doped and Codoped Tio_2

IV. CONCLUSION PAGE STYLE

The uniform and fineness nanoparticles of undoped and cobalt doped TiO_2 are prepared by simple and cheap sol-gel method. All the samples have almost similar structure. XRD has also been used to analyse various parameters like SSA, dislocation density and morphology index to explore the importance of nano-particles. The band gap can be

tuned with doping as per requirement of any optical devices

ACKNOWLEDGMENT

Author would like to acknowledge sophisticated analytical instrumentation facility, Panjab University, Chandigarh, to access the equipment for characterization and Kurukshetra University Kurukshetra for financial support through miner research project.

REFERENCES

[1] B. Bharti, P. B. Barman and Rajesh Kumar, "XRD analysis of undoped and Fe doped TiO2 nanoparticles by Williamson Hall method," AIP Conf. Proc., vol.1675, pp. 030025, 2015, doi: 10.1063/1.4929241.

[2] R. Mechiakh and R. Bensaha, "Variation of the structural and optical properties of sol–gel TiO2 thin films with different treatment temperatures," C. R. Physique, vol. 7, 2006, pp.464.

[3] J. R. Simpson and H. D. Drew, "Optical band-edge shift of anatase $Ti_{1-x}Co_xO_2$," Phy. Rev. B, vol. 69, pp. 193205, 2004.

[4] S. Guha, K. Ghosh, J. G. Keeth, S. B. Ogale, S. R. Shinde, J. R. Simpson, H. D. Drew, and T. Venkatesan, "Temperature-dependent optical studies of $Ti_{1-x}Co_xO_2$,'' Appl. Phys. Lett. vol.83, pp. 3296, 2003.

[5] Y. Chen, G. Zhao, Y. Ren and Z. Wang, "Microfabrication of dilute magnetic semiconducting Ti1−xCoxO2 films using photosensitive sol–gel method," Thin Solid Films, vol. 519, pp.1985, 2011.

[6] K. Siddhapara and D. Shah, "Characterization of nanocrystalline cobalt doped TiO_2 sol–gel material," J. Crys. Grow. vol.352, pp. 224 2012.

[7] K. Karthik, S. Kesava Pandian, K. Suresh Kumar and N. Victor Jaya, "Influence of dopant level on structural, optical and magnetic properties of Co-doped anatase TiO_2 nanoparticles," Appl. Surf. Sci. vol. 256, pp. 4757, 2010.

[8] M. Guo, Y. Gao and G . Shao, "Complex doping chemistry owing to Mn incorporation in nanocrystalline anatase TiO2 powders," Phys.Chem.Chem.Phys., vol.18, pp. 2818, 2016.

[9] S. A. Ahmed, "Annealing effects on structure and magnetic properties of Mn-doped TiO2," J. Magn. Magn. Mater. vol.402, pp.178, 2016.

[10] G. Rana, U.C. Johri and K. Asokan, "Correlation between structural and dielectric properties of Ni-substituted magnetite nanoparticles," Euro. Phys. Lett. vol.103, pp.17008, 2013.

[11] B. Santara, B. Pal and P. K. Giri, "Signature of strong ferromagnetism and optical properties of Co doped TiO2 nanoparticles," J. Appl. Phys. vol.110, pp.114322, 2011.

[12] G. K.Williamson and W. H. Hall, "X-Ray line broadening from filed Aluminium and Wolfram, Acta Metallur. vol.1, pp.22, 1953.

[13] A. K. Zak, W. H. A. Majid, M .E. Abrishami and R. Yousefi, "X-ray analysis of ZnO nanoparticles by Williamson Hall and size strain plot," Solid State Sci. vol.13, pp.251, 2011.

[14] R. R. Prabhu and M .A. Khadar, "Study of optical phonon modes of CdS nanoparticles using Raman Spectroscopy," Bull. Mater. Sci. vol.31, pp.511, 2008.

[15] V. Senthilkumar, P. Vickraman, M. Jayachandran and C. Sanjeeviraja, "Structural and electrical studies of nano structured Sn_{1-x} Sb_xO_2 (x= 0.0, 1, 2.5, 4.5 and 7 at%) prepared by co-precipitation method," J. Mater. Sci.: Mater. Electron. vol.21, pp.343, 2010.

[16] A. J. Antony, J. Nutting, D. R. Baer, D. Meyer, A. Sharma and Y. Qiang, "Size-Dependent Specific Surface Area of Nanoporous Film Assembled by Core Shell Iron Nanoclusters," J. Nanomaterials, vol. 2006, pp. 1, DOI 10.1155/JNM/2006/54961.

[17] J. Zhang, X. Xiao and J. Nan, "Hydrothermal-hydrolysis synthesis and photocatalytic properties of nano-TiO_2 with an adjustable crystalline structure," J. Haz. Mat. vol. 176, pp. 617, 2010.

[18] S. Velumani , X. Mathew, P. J. Sebastian, S. K. Narayandass and D. Mangalaraj, "Structural and optical properties of hot wall deposited CdSe thin films," Solar Energy Mater. Solar cells. vol.76 , pp.347, 2003.

[19] N. Q. Chinh, J. Gubicza and Langdon, "Characteristics of face-centered cubic metals processed by equal-channel angular pressing," T G. J. Mater. Sci. vol.42, pp.1594, 2007, DOI 10.1007/s10853-006-0900-3.

[20] T. P. Yendrapati., V. R. Kalagadda, S. S. K.Vemula, S. K. Bandla, "Synthesis of ZnO Nanoparticles by a Novel Surfactant Assisted Amine Combustion Method," Adv. in Nanoparticles, vol.2, pp. 45, 2013, http://dx.doi.org /10.4236/ anp.2013.21009.

[21] Q. Hua, J. Huanga, G. Lia, Y. Jianga, H. Lana, W. Guoa and Y. Cao, "Origin of the improved photocatalytic activity of Cu incorporated TiO2 for hydrogen generation from water," Appl. Surf. Sci. vol. 382, pp.170, 2016.